Cell Transplantation, Vol. 25, pp. 2199–2211, 2016
Printed in the USA.

0963-6897/16 $90.00 + .00
DOI: http://dx.doi.org/10.3727/096368916X692104
E-ISSN 1555-3892
www.cognizantcommunication.com

Long-Term Cell Tracking Following Local Injection of Mesenchymal Stromal Cells in the Equine Model of Induced Tendon Disease

Janina Burk,*†‡ Dagmar Berner,§ Walter Brehm,*†§ Aline Hillmann,*† Carolin Horstmeier,*†§ Christoph Josten,¶ Felicitas Paebst,§ Giacomo Rossi,# Susanna Schubert,*† and Annette B. Ahrberg*†¶

*Saxon Incubator for Clinical Translation (SIKT), University of Leipzig, Leipzig, Germany
†Translational Centre for Regenerative Medicine (TRM), University of Leipzig, Leipzig, Germany
‡Institute of Veterinary Physiology, University of Leipzig, Leipzig, Germany
§Large Animal Clinic for Surgery, University of Leipzig, Leipzig, Germany
¶Department of Orthopedics, Traumatology and Plastic Surgery, University of Leipzig, Leipzig, Germany
#University of Camerino, School of Biosciences and Veterinary Medicine, Matelica (MC), Italy

Tendon disease has been treated with multipotent mesenchymal stromal cells (MSCs) in the equine large-animal model with promising success. The aim of this study was to gain more insight into the fate and biodistribution of MSCs after local application into tendon lesions by long-term cell tracking in this large-animal model. Superficial digital flexor tendon lesions were induced in all limbs in six horses and injected with 10×10^6 Molday ION Rhodamine B™-labeled MSCs suspended in serum or serum alone. Follow-up was performed using low-field magnetic resonance imaging (MRI), flow cytometry, and histology. Cell tracking based on the hypointense artifacts induced by the superparamagnetic iron oxide (SPIO) labeling agent in MRI as well as based on Rhodamine B fluorescence was feasible. However, Prussian blue staining for assessment of histology was not entirely specific for SPIO. Labeled cells could be traced at their injection site by MRI as well as histology for the whole follow-up period of 24 weeks. Although the numbers of labeled cells within the injected tendon lesions decreased over time, part of the applied cells appeared to remain viable and integrated within the injured tissue. Furthermore, small numbers of labeled cells were identified in peripheral blood within the first 24 h after cell injection and could also be found until week 24 within the contralateral control tendon lesions that had been injected with serum. The present findings unveil details on MSC biodistribution and persistence after their local application, which are of clinical relevance with regard to MSC safety and mechanisms of action.

Key words: Tendon; Mesenchymal stromal cells (MSCs); Cell therapy; Cell tracking; Biodistribution; Superparamagnetic iron oxide (SPIO)

INTRODUCTION

Treatment of tendon disease is one of the highly promising options within the large field of potential clinical applications of multipotent mesenchymal stromal cells (MSCs). Studies performed in the equine species led to results that encourage further investigation (14,30,34). The horse is considered a natural model for tendon disease, as the etiopathogenesis of equine superficial digital flexor tendon and human Achilles tendon disease shows several similarities (26,28). Providing a basis for further translation of the therapeutic concept, the use of the equine large-animal model for preclinical orthopedic research has been recommended in the guidelines issued by authorities such as the US Food and Drug Administration (FDA) and the European Medicines Agency (EMA) (18,37). With respect to using the horse not only for orthopedic but also for cell therapy research, we recently demonstrated a high level of analogy of equine and human MSCs (22), enabling the use of the horse in homologous models for cell therapies.

The approach previously used in the horse for cell therapy for tendon disease is based on the local, ultrasound-guided application of an MSC suspension. This was first published more than a decade ago (32) and has since then been shown to improve the tendon tissue architecture after injury (14,30,34). However, despite growing evidence regarding the efficacy, fundamental questions remain regarding the fate of the applied MSCs as well as their mechanism of action.

Previous studies that have been performed in order to track MSCs applied for treatment of tendon injuries

Received December 23, 2015; final acceptance September 7, 2016. Online prepub date: July 7, 2016.
Address correspondence to Dr. Janina Burk, Saxon Incubator of Clinical Translation (SIKT), University of Leipzig, Philipp-Rosenthal-Str. 55, 04103 Leipzig, Germany. Tel: +49-341-9739616; Fax: +49-341-9738269; E-mail: burk@rz.uni-leipzig.de

already give some insight into the fate and biodistribution of the cells. However, it is still difficult to assemble a comprehensive picture. In studies using the equine model and local application of MSCs transfected with green fluorescent protein (GFP), the cells could mainly (19,20) or exclusively (21) be found at their injection site by histological assessment. While giving good insight into MSC integration within the tissue microstructure, this technique is limited with regard to longitudinal cell tracking and detection of potential systemic MSC distribution in the large-animal model. Only low percentages such as <1% of the total injected MSCs could be found in tissue sections obtained 60 or 90 days after MSC application in this study, leading to the hypothesis of limited survival of the cells (21). Contrary to these results, in a similar study design using a sheep model and local application of red fluorescent protein (RFP)-transfected MSCs, persistence of labeled MSCs was observed in the injected tendon lesions until 6 weeks after application (25). However, corresponding to the earlier study, no evidence of MSC migration and homing to distant locations was found in this study either (25).

A different approach with contrary advantages and disadvantages also being used in large-animal models is scintigraphic tracking of technetium-99-labeled MSCs (5,36). Here the major limitations are the short persistence and detectability of cell labeling as well as the low spatial resolution. However, scintigraphic tracking can be used for monitoring cells in vivo and offers the best currently available opportunity to assess MSC biodistribution in large-animal species, at least over a short period of time. It also represents a possible technique for quantification of cell numbers, although the rapid loss of label remains an issue. So far, scintigraphy was mainly used to investigate alternative delivery routes for MSC treatment of tendon lesions, such as systemic intravenous injection or regional perfusion. Different studies consistently led to the result that direct intralesional injection of MSCs results in higher uptake within the lesion compared to regional perfusion (5,36), making this delivery route still appear most favorable. Nevertheless, regional perfusion as well as a single case of systemic intravenous injection also led to measurable uptake within the tendon lesion (5), suggesting homing of applied MSCs to injured regions, albeit with inadequate and inconsistent efficiency.

Adding to the question of potential homing, in a further study using quantum dot labeling, MSCs could be detected histologically in locally injected tendon lesions, but not in contralateral control tendon lesions after 7 days (12). However, in the same study, distribution of labeled cells in the peripheral blood was observed by flow cytometry, leading to the assumption they may have distributed to other parts of the body.

Taking these previous findings together, although there is evidence that local administration of MSCs is the method of choice for cell treatment of tendon disease, long-term intratendinous persistence and biodistribution of the MSCs are still not elucidated. Therefore, alternative techniques suitable for longitudinal cell tracking should be an area of focus.

Magnetic resonance imaging (MRI) may be a suitable tool for in vivo cell tracking studies. The use of modern high-field magnets in small animals results in high-resolution images revealing detailed information (2). Furthermore, albeit with lower resolution, MRI cell tracking is also feasible in large animals. MRI contrast agents for intracellular labeling such as superparamagnetic iron oxide (SPIO) particles were shown to have no or low impact on in vitro cell properties (1,7,13,23) and persist in the cells for several weeks (7,15). SPIO particles lead to local magnetic field perturbations and can therefore be visualized as signal void susceptibility artifacts in MRI. Furthermore, SPIO-labeled cells stain positive for Prussian blue, potentially facilitating additional assessments by histology.

Recently, MRI has been described for in vivo cell tracking in induced tendon lesions in an ovine model (29). This study provided data on a limited follow-up time of 2 weeks but demonstrated that Prussian blue-positive histology staining was present within areas of the tendon lesions that corresponded well to the signal void areas in the MR images. Furthermore, using MSCs that had been transducted with green fluorescent protein and colabeled with SPIO, the presence of viable, labeled cells could be confirmed histologically (29).

We recently published the results of low-field MRI cell tracking over 8 weeks after treatment of tendon lesions in equine patients (6), demonstrating the feasibility of this technique in horses. The availability of an equine-dedicated low-field MRI system offers the advantage that the animals do not require general anesthesia during the examinations, which facilitates monitoring at close intervals. In this study, tracking over 8 weeks provided new insight in terms of longer follow-up as well as SPIO-artifact localization in naturally occurring tendon disease. However, because the animals were client-owned patients, no tissue samples could be harvested, impairing histological assessment. Adding to this patient study, a recent experimental pilot study in horses confirmed that MSC tracking in tendon lesions by low-field MRI is feasible over a period of 9 weeks, while labeled cells could also be found histologically (19).

The aim of the current study was to perform longitudinal cell tracking, combining in vivo MRI and histological assessment over a significant period of time, for which we chose a follow-up time of 24 weeks. Furthermore, we aimed to gain insight not only into the local distribution

of MSCs applied to induced tendon lesions but also into the potential systemic distribution and homing of MSCs to other injury sites. For this purpose, MSC labeling with SPIO particles conjugated to Rhodamine B was chosen to allow detection of cells by MRI and Prussian blue staining as well as fluorescence-based microscopy and flow cytometry, enabling comprehensive analysis of different types of samples.

MATERIALS AND METHODS

Animals and Induction of Tendon Lesions

Six healthy Standardbred horses (3–10 years; three females, three males) were used for this study. Horses were examined clinically and by ultrasonography as well as MRI of the metacarpal or metatarsal flexor tendons to rule out preexisting tendon disease prior to including the animals in the study. All procedures were approved by the local authority (Landesdirektion Leipzig, TV 34/13).

Tendon lesions were induced in the mid-metacarpal/mid-metatarsal region of the superficial digital flexor tendons in all four limbs (17) by combining a surgical procedure with collagenase application. Horses were placed in lateral recumbency under general anesthesia, and the skin was prepared aseptically. Tendon lesions were induced by introducing an 11-gauge multiport bone marrow aspiration needle through a 2-cm proximodistal skin incision. The needle was advanced within the tendon for a distance of 2 cm to proximal, then 0.4 ml of 4.8 mg/ml (250 IU per tendon lesion) collagenase I (Life Technologies GmbH, Darmstadt, Germany) solution was applied while slowly drawing the needle back. Subcutis and skin were closed by continuous suture and simple interrupted pattern, respectively, and bandages were applied. Following the induction of tendon lesions, autologous subcutaneous adipose tissue was collected from the supragluteal region for isolation of autologous MSCs as described previously (8). All animals were administered flunixin meglumine (Flunidol®; CP-Pharma Handelsgesellschaft mbH, Burgdorf, Germany) as a nonsteroidal anti-inflammatory drug [pre- and 10 h postsurgery: 1.1 mg/kg body weight (bwt) intravenously (IV); day 1 to day 4 postsurgery: 0.55 mg/kg bwt per oral administration (PO) twice daily; day 5 to day 6 postsurgery: 0.55 mg/kg bwt PO once daily]. They were monitored at least three times daily for 10 days using a pain score, which allowed standardized additional treatment if required. Single additional doses of pain medication (flunixin meglumine, 1.1 mg/kg bwt PO) were administered according to the standardized regime when an animal showed signs of discomfort or pain. The limbs were left bandaged for 14 days when the skin sutures were removed.

After surgery, horses were restricted to stall rest until 2 weeks after MSC application. Thereafter, they were subjected to a standardized, gradually increasing exercise program for tendon rehabilitation described previously (33).

MSC Isolation, Labeling, and Characterization

Mononuclear cells (MNCs) were isolated from the adipose tissue collected after the induction of tendon lesions by collagenase I digestion as described previously (10). The plastic-adherent MSC fraction was expanded until passage 2.

MSCs were then labeled with Molday ION Rhodamine B™ (BioPAL Inc.™, Worcester, MA, USA) at an iron concentration of 25 μg Fe/ml culture medium at 37°C in humidified atmosphere for 20 h. Following labeling, MSCs were harvested, and 10×10^6 cells per tendon lesion to be treated were suspended in 1 ml of fresh autologous proband serum. Remaining labeled cells from each animal were used for the evaluation of labeling and trilineage differentiation potential. For evaluation of labeling, MSCs were reseeded and incubated for 24 h for cell attachment, and intracellular iron particles were stained with the Prussian Blue Reagent Pack (BioPAL Inc.™) according to the manufacturer's instructions. The percentage of Prussian blue-positive cells was assessed quantitatively by light microscopy in at least one 10× field of view per sample. In addition to that, the percentage of Rhodamine B-positive MSCs was assessed by flow cytometry as described below. Trilineage differentiation and subsequent stainings were performed as described previously (10,22). Briefly, Oil red O staining was performed to detect lipid droplets and von Kossa staining to detect mineralizations, and Alcian blue and Masson's trichrome staining were used to demonstrate glysosaminoglycan and collagen deposition, respectively. Staining reagents were obtained from Carl Roth (Karlsruhe, Germany) and Sigma-Aldrich (Munich, Germany). Oil red O and von Kossa staining were combined with Prussian blue staining to detect remaining labeling agent after differentiation.

Furthermore, nonlabeled passage 2 cells from each animal were used for characterization of MSC surface antigens by flow cytometry. Immunostaining comprised staining of the putative positive markers CD29, CD 44, CD73, CD90, and CD105 and staining of the putative exclusion markers CD14, CD34, CD45, CD79α, and major histocompatibility complex (MHC) II. Primary antibodies were purchased from BioLegend (CD29; San Diego, CA, USA), Becton Dickinson (CD44; Franklin Lakes, NJ, USA), Abcam (CD73; Cambridge, UK), R&D Systems (CD90 and CD14; Minneapolis, MN, USA), Serotec (CD105, CD45, CD79α, and MHC II; Kidlington, UK), and Santa Cruz Biotechnology (CD34; Santa Cruz, CA, USA). All antibodies and antigen subsets were chosen on the basis of previous studies, and staining as well as analysis procedures were performed accordingly (22,27).

MSC Injection

Three weeks after induction of tendon lesions and adipose tissue collection, one randomly chosen forelimb and one randomly chosen hindlimb tendon lesion of each horse were injected locally with 10×10^6 labeled MSCs in 1 ml of autologous serum, while the respective contralateral tendon lesions were injected with 1 ml of serum only. The injections were performed in the standing sedated horses after perineural (ulnar nerve or lateral and medial plantar nerves) and local anesthesia using lidocain 2% (Bela-pharm GmbH & Co. KG, Vechta, Germany). All injections were performed by the same qualified veterinary surgeon unaware of the presence of MSCs in the respective syringes. In the weight-bearing limb, a 20-gauge needle was placed perpendicular to the tendon axis and advanced into the lesion. Intralesional placement of the needle was monitored by ultrasonography using a 10-MHz linear transducer (LOGIQ 5 Expert; GE Healthcare, Munich, Germany) before MSCs or serum was applied. After the injection, the limbs were bandaged for 2 days. All animals were administered flunixin meglumine at the day of injection (1.1 mg/kg bwt IV) as well as the following day (0.55 mg/kg bwt PO).

Longitudinal Cell Tracking by MRI

MRI examinations were performed at regular intervals in order to track the labeled MSCs longitudinally in vivo. T1-weighted and T2*-weighted gradient echo MRI series [slice thickness: 5 mm; gap: 1 mm; field of view: 171 mm × 171 mm; matrix: 256 × 256; repetition time (TR), T1w: 52 ms; TR, T2*w: 68 ms; echo time (TE), T1w: 8 ms; TE, T2*w: 13 ms; flip angle, T1w: 50°; flip angle, T2*w: 25°] were acquired in a transverse plane using an equine-dedicated low-field MRI system (EQ2; Hallmarq Veterinary Imaging, Guildford, Surrey, UK) for examinations in standing sedated horses as described previously (6). Examinations of all four limbs were performed directly before and after MSC application as well as 1, 2, and 3 weeks after MSC application. The MRI scans after MSC application were started immediately after the injection and completed within 4 h. After the hindlimb biopsies had been collected at week 3, MRI examinations included the forelimbs only and were repeated 4, 6, 8, 12, and 24 weeks after MSC application.

MRI series were evaluated regarding the localization and dimension of the putatively iron oxide-induced hypointense artifacts over time using Synedra ViewPersonal, Version 3.4.0.2 (Synedra Information Technologies GmbH, Innsbruck, Austria). Localization was categorized as intratendinous, predominantly intratendinous, equally intratendinous and within surrounding tissue, predominantly within surrounding tissue, or within surrounding tissue. Artifact dimension was approximated by measuring its area in all consecutive images and multiplying the sum of artifact areas by 6 mm (5-mm slice thickness + 1-mm gap). Measurements were repeated three times, and mean values were used for further analysis.

Sample Collection for Flow Cytometry and Histology

Three weeks after cell application, 0.2-cm × 0.3-cm × 2-cm tendon biopsies were recovered from the hindlimb maximum lesion and injection sites from all six horses under general anesthesia. Pain management was performed as described above for the induction of tendon lesions. Biopsies were collected from the core of the tendon lesions via skin incision and using a scalpel to recover the sample piece under visual control. Tendon, subcutis, and skin were sutured, and the limbs were bandaged. Each hindlimb biopsy was divided into two parts. One part was fixed in 4% paraformaldehyde (PFA; Carl Roth) and subjected to histology. From the other part, cells were released by digestion in 5.6 mg/ml collagenase solution for 6 h at 37°C and subjected to flow cytometry.

Twenty-four weeks after cell application, all six horses were sacrificed, and the whole metacarpal regions of the forelimb tendons were collected. The tendons were divided into 2-cm-long sample pieces by transverse cutting, the most proximal piece corresponding to the proximal aspect of the metacarpal region, and the most distal piece to the distal aspect of the metacarpal region. A central part of each 2-cm piece was fixed in 4% PFA and subjected to histology.

Additional samples were collected from three of the animals (male; 5–9 years) to assess potential systemic distribution of MSCs as well as potential homing to other injury sites: 30 ml of peripheral blood samples was collected 1 h before and 1, 4, 8, 12 h, as well as 1, 2, 3, 4, 5, and 6 days after MSC injection. MNCs in the blood samples were purified by density gradient centrifugation at $327 \times g$ (27) and assessed by flow cytometry. In addition to the tendon biopsies, at week 3 after cell application, 0.5-cm-diameter biopsies were collected from healthy and previously injured subcutaneous and muscle tissue. Previously injured tissue was taken from the (supra)gluteal region at the site where adipose tissue had been harvested, and healthy tissue was taken from the same (supra)gluteal region but in a distance of 30 cm to the previous incision for adipose tissue harvest. Corresponding control biopsies were collected from two different horses, which had not been included in the study procedures before. These two animals had never received labeled MSCs but had undergone the same surgical procedure for adipose tissue harvest the same

period of time ago. The biopsies were fixed in 4% PFA and subjected to histology.

Flow Cytometry

Freshly labeled MSCs as well as MNCs recovered from the peripheral blood samples were stained with Fixable eFluor 780® (eBioscience, Frankfurt a.m., Germany) for exclusion of dead cells in flow cytometry. Stained labeled and unstained nonlabeled control cells were fixed with 2% PFA. Rhodamine B fluorescence of live cells was analyzed using a FACSCanto II (Becton Dickinson). For blood samples, a minimum of 5×10^6 events was recorded. Rhodamine B fluorescence of cells released from the tendon biopsies was analyzed without previous cell fixation using a FACSAria III™ (Becton Dickinson). Data analysis was performed with FlowJo software version 10.0.7 (FlowJo LLC, Ashland, OR, USA).

Histology

All biopsies obtained at week 3 as well as all samples obtained from the whole forelimb tendons at week 24 were processed into 3-µm paraffin sections. Two nonadjacent sections from each sample were subjected to Prussian blue staining with nuclear fast red (Sigma-Aldrich) counterstaining, while two corresponding sections were subjected to 4′,6-diamidino-2-phenylindole (DAPI; Carl Roth) counterstaining of nuclei. Whole slide images of each section were obtained in a slide scanner (Pannoramic SCAN; 3DHISTECH, Budapest, Hungary) and were used for the evaluation of histology. The presence of fibroblast-like structures displaying Prussian blue staining was quantified by two blinded, independent observers. Furthermore, corresponding DAPI-stained sections were evaluated with regard to the presence of Rhodamine B-positive cells. Representative sections of MSC- and serum-injected tendon lesions were additionally examined with an inverted confocal laser scanning microscope TCS SP5 (Leica Microsystems, Wetzlar, Germany). To avoid cross talk in excitation of 375 and 561 nm in multiple-stained compounds, a sequential scanning mode was executed. Images were analyzed with the software Leica Application Suite Advanced Fluorescence 2.6.0 (Leica Microsystems) and Adobe Photoshop CS (Adobe Systems, Munich, Germany).

Statistical Analysis

Data are presented as median and interquartile range (IQR). Statistical analysis was performed using SPSS Statistics 22 software (IBM Deutschland GmbH, Ehningen, Germany). As not all data were evenly distributed, for comparisons between paired groups, Wilcoxon tests were performed. Differences were considered significant at $p < 0.05$.

RESULTS

Tendon Lesions and Surgeries

The technique for tendon lesion induction led to reproducible core lesions that had largely the same appearance as natural equine tendon lesions in ultrasonography, MRI, and histology (unpublished data). The surgeries for tendon lesion induction and biopsy sampling were generally tolerated well, although the latter caused obvious additional injury. During the first days after surgery, the animals showed mild to moderate signs of pain, which were manageable with the flunixin meglumine treatment specified above. During the rest of the study period, the animals did not show signs of pain or discomfort related to the surgeries, except for initial mild lameness, which decreased and disappeared after the first few weeks.

MSC Characterization and Labeling

The isolated cells were positive for CD29 [61.9% (IQR: 55.4%)], CD44 [IQR: 90.6% (IQR: 14.1%)], CD90 [6.5% (IQR: 29.6%)], and CD105 [25.6% (IQR: 15.3%)] and showed no or less than 2.0% expression of CD73, CD14, CD34, CD45, CD79α, and MHC II.

Labeling with Molday ION Rhodamine B was confirmed to be highly efficient. Evaluation by light microscopy showed that 100.0% (IQR: 2.7%) of MSCs were Prussian blue positive (Fig. 1). Flow cytometry led to corresponding results, with 99.8% (IQR: 0.4%) Rhodamine B-positive cells.

Furthermore, labeled MSCs from all animals showed trilineage differentiation potential, showing intracellular lipid droplets after adipogenic induction, extracellular mineralized matrix after osteogenic induction, as well as glycosaminoglycan and collagen deposition (data not shown) after chondrogenic pellet culture (Fig. 1).

Persistence of labeling particles during MSC differentiation was distinct in the chondrogenic pellet cultures, which all displayed marked brownish accumulations in close proximity to the cell nuclei after the incubation time of 21 days. In contrast, Prussian blue-positive staining could only be observed in few single cells after 7 days of monolayer culture and adipogenic differentiation, and no Prussian blue-positive cells were found after osteogenic induction in monolayer culture for 21 days (Fig. 1).

Longitudinal MRI Cell Tracking

After the injection of labeled MSCs, hypointense artifacts were visible in T1- and T2*-weighted MR images. These artifacts remained present in the MSC-injected limbs of all animals until week 24, while no such artifacts had been visible before the injection of MSCs (Fig. 2). Furthermore, no distinct artifacts were observed in the contralateral limbs.

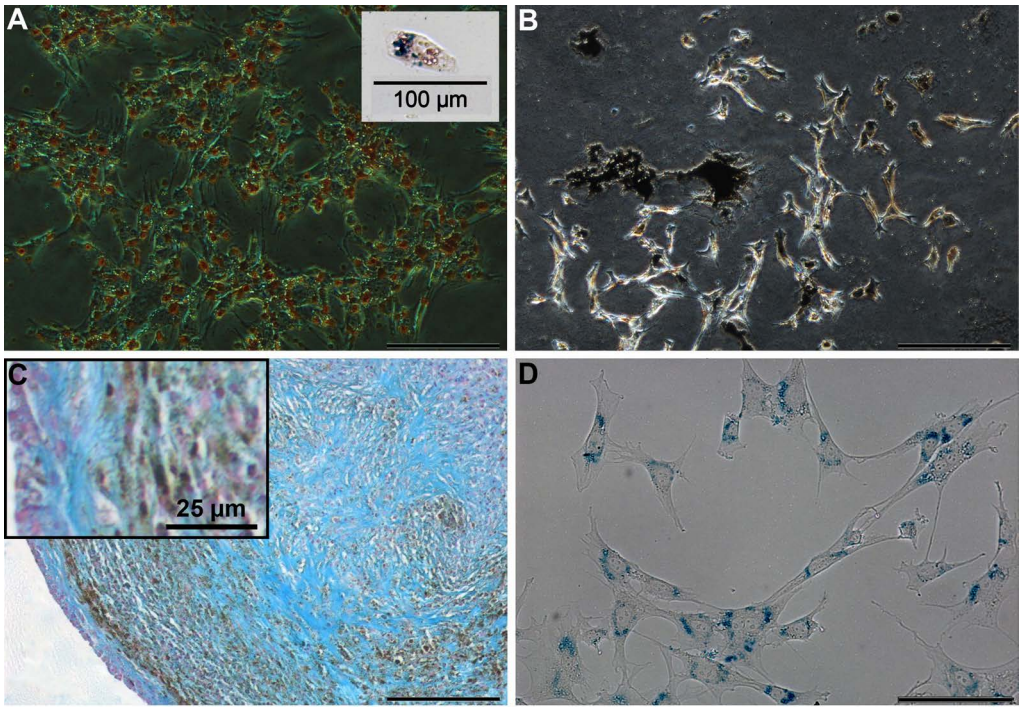

Figure 1. MSC differentiation and labeling. Representative images of trilineage differentiation of labeled MSCs. (A) Oil red O staining of lipid droplets after adipogenic induction, the inset displaying one of the few cells still staining positive for Prussian blue after adipogenic differentiation. (B) von Kossa staining of mineralizations after osteogenic induction. (C) Alcian blue staining of glycosaminoglycans after chondrogenic pellet culture; note the brownish iron oxide accumulations in areas of high cellularity. (D) Prussian blue staining of the intracellular iron oxide particles in undifferentiated, freshly labeled MSCs. Scale bars: 200 µm, unless marked otherwise.

The volume of the artifacts present within the limbs gradually decreased over time and was significantly lower at week 12 and week 24 compared to the earlier examinations in both T1- and T2*-weighted sequences ($p<0.05$) (Fig. 2). Furthermore, while showing a similar decreasing trend, the volume of the hindlimb artifacts was lower compared to the forelimbs, which was significant in T1-weighted images at weeks 1, 2, and 3 ($p<0.05$).

After cell application, artifacts were localized intratendineously as well as within the surrounding tissue in 11 out of 12 limbs. In the remaining limb, the artifact was found only in the surrounding tissue. In one further limb, artifact localization shifted from intratendineous to the surrounding tissue during the first week of follow-up. However, in all other cases, the artifacts constantly remained intratendineous, and their localization even became more central within the lesion over time in 3 out of 12 limbs.

Labeled Cells in Peripheral Blood

Flow cytometry could detect small numbers of Rhodamine B-positive cells within the peripheral blood-derived mononuclear cells (PB-MNCs), indicating distribution of labeled MSCs with the circulating blood. Numbers of detectable Rhodamine B-positive cells varied between animals, but the highest cell numbers over time were consistently found within the first 24 h after MSC injection. Maximum Rhodamine B-positive cell counts ranged from 9,079 per 10^6 cells at 8 h postinjection in one animal to 513 and 304 per 10^6 cells at 12 h postinjection in the other two animals. After reaching these respective maxima, the numbers of Rhodamine B-positive cells decreased. In the latter two animals, no more labeled cells were detected after 2 days, while in the first animal, cell numbers ranging from 234 to 569 per 10^6 cells remained detectable until day 6.

Labeled Cells in Tissue Samples

Prussian blue-positive staining could be observed in tissue sections of the tendon injury site prepared at week 3 as well as week 24 after MSC application. The staining partly occurred as blue specks of undefined shapes but was mostly associated with cell nuclei and displayed defined, fibroblast-like shapes. This was evident not only in the tendons injected with labeled MSCs but also in the contralateral tendon lesions (Fig. 3) as well as in the injured subcutaneous and muscle tissue. However, importantly, although in lower quantities, similar occurrence of Prussian blue staining was found in the control injured subcutaneous

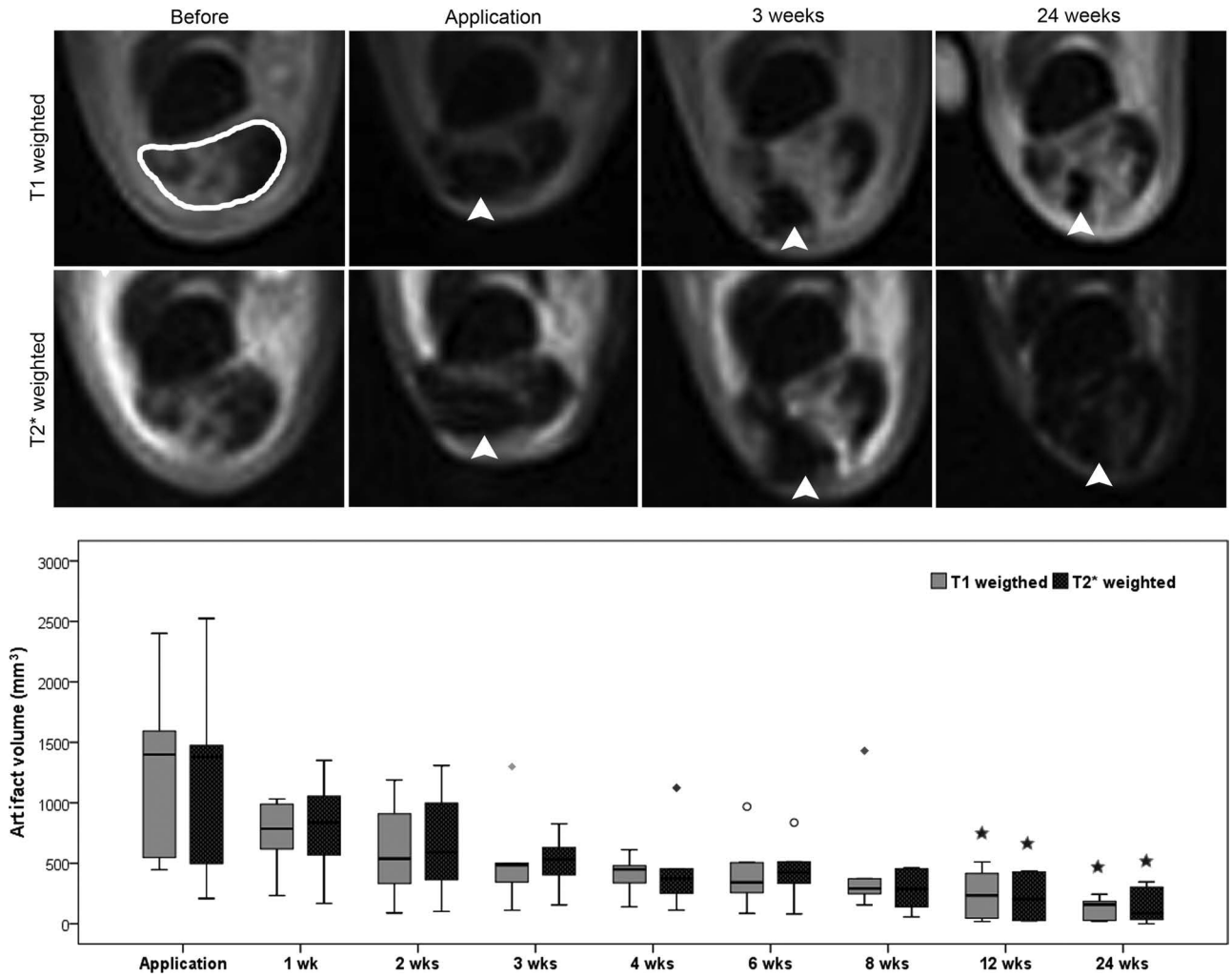

Figure 2. MRI cell tracking. Representative images of T1- and T2*-weighted gradient echo MRI sequences before and at different time points after cell application, and boxplot displaying the artifact volume over time. Left upper image: the superficial digital flexor tendon with its hyperintense lesion is indicated by the white line. Arrows point at the hypointense artifact putatively induced by the iron oxide-labeled MSCs. Note that the artifact becomes smaller over time, as also demonstrated by the decreasing artifact volume. Boxplot: circles and rhombs display outliers, and stars indicate significant differences compared to the earlier time points ($p < 0.05$).

and muscle tissue samples of the animals that had never received labeled MSCs (Fig. 4). In contrast, in sections of healthy tendon recovered distal or proximal to the injury site or sections of healthy subcutaneous and muscle tissue, Prussian blue staining was negative.

Prussian blue-positive fibroblast-like structures within the tendon samples were present in higher numbers at week 3 compared to week 24 after MSC application. Furthermore, while the numbers obtained at week 3 were similar in injected and contralateral tendons, at week 24 higher numbers were found in the tendon lesions injected with labeled MSCs compared to the contralateral lesions (Fig. 3). However, these differences were not significant.

More specific assessment on the basis of Rhodamine B labeling revealed that Rhodamine B-positive cells were actually present in the MSC-injected as well as in the contralateral tendon lesions in all animals. However, the presence of equal numbers of labeled cells in both MSC-injected and contralateral tendon lesions at week 3, as suggested by Prussian blue staining, could not be confirmed, neither microscopically nor by flow cytometry. Rather, flow cytometry at week 3 revealed that in the MSC-injected lesion, 2.5% (IQR: 3.1%) of total cells recovered from the maximum lesion site were Rhodamine B positive, while in the contralateral lesion lower numbers of cells [0.5% (IQR: 0.5%)] were positive (Fig. 5). However, the cell numbers found in the MSC-injected lesion were variable, as demonstrated by the comparatively high IQR; thus, the difference between MSC-injected and contralateral lesion was not significant.

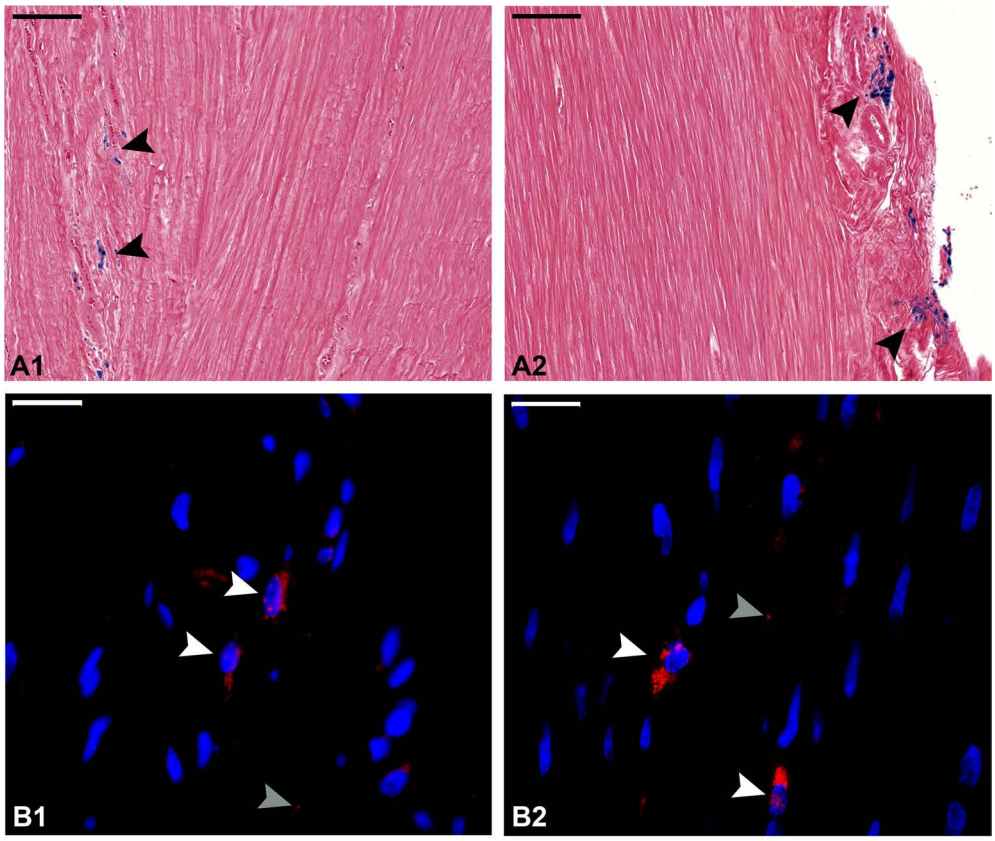

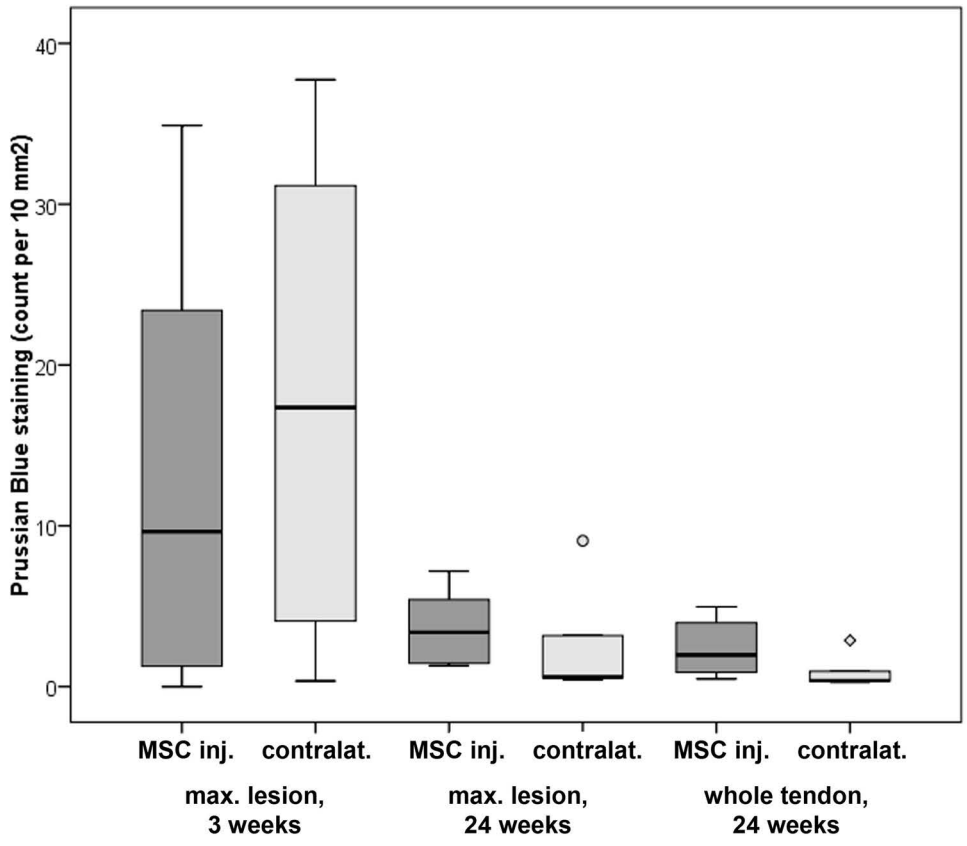

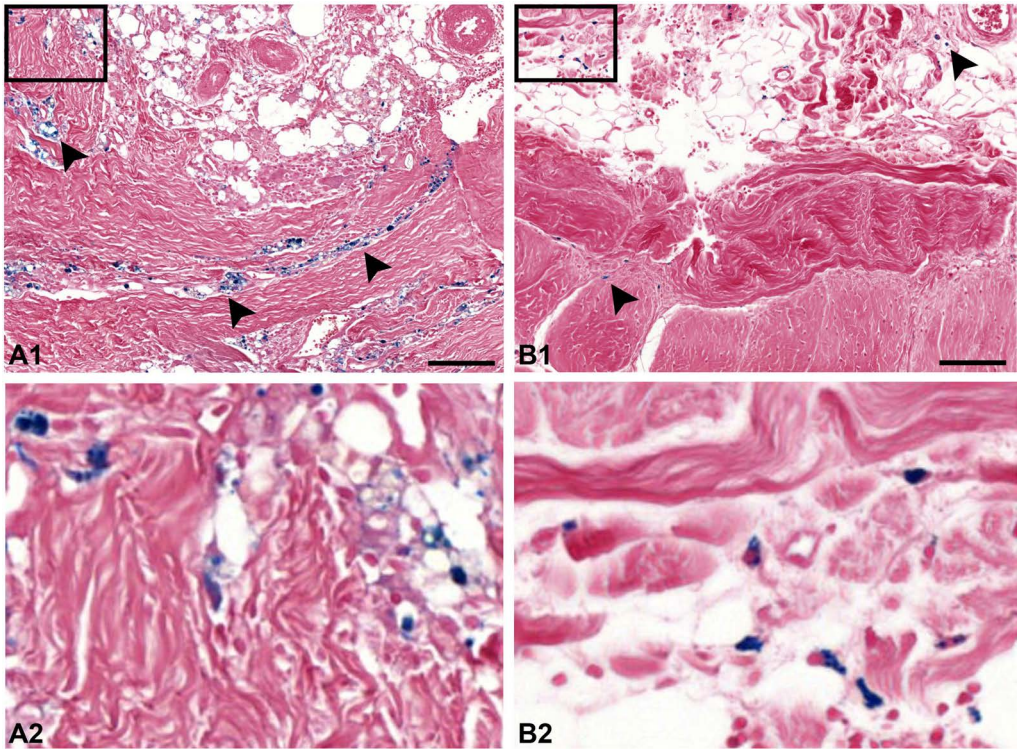

Figure 4. Prussian blue staining in scar tissue. Muscle and subcutaneos scar tissue obtained 6 weeks after injury (A) displaying extensive Prussian blue staining (arrows) in an animal that had received an intratendineous injection of iron oxide-labeled MSCs 3 weeks before the biopsy was taken and (B) displaying moderate Prussian blue staining in an animal that had never received labeled MSCs. Scale bars: 100 μm. The rectangles in (A1) and (B1) mark the areas displayed in higher magnification in (A2) and (B2).

Prussian blue- as well as Rhodamine B-positive cells were predominantly localized in groups within the enlarged endo- and peritenon, often in close proximity to blood vessels, or aligned between nonmature tendon fibers. Furthermore, additional Prussian blue staining with undefined shapes was observed in most samples obtained from tendon lesions, which was partly reflected by an occasional occurrence of single Rhodamine B-positive particles (Fig. 3).

DISCUSSION

In this study, we performed the first long-term longitudinal cell tracking in a large-animal model of tendon disease, aiming to gain insight into local persistence as well as potential systemic distribution of locally applied MSCs. We found evidence that part of the labeled cells remained at the local injection site for the whole follow-up period of 24 weeks. However, our results also suggest that a limited and variable number of locally injected cells is distributed via the blood circulation and relocates to other injury sites.

Finding reliable techniques for tracking of transplanted cells is still challenging, and it is inevitable to deal with their limitations. We aimed to combine different approaches to overcome part of these limitations but still faced some issues that should be considered.

MRI is an advantageous technique for long-term tracking as it is noninvasive and can therefore be used to obtain valuable information over time. At the same time, MRI cell tracking has some obvious limitations. First, the

FACING PAGE

Figure 3. Histology of tendon lesions. Representative images of tendon lesion histology obtained 24 weeks after MSC application and boxplot displaying the numbers of Prussian blue-positive, fibroblast-like structures in tissue sections obtained from the maximum lesion site at week 3 and week 24 as well as mean values of all tissue sections obtained from each tendon at week 24. (A) Prussian blue staining potentially indicating presence of iron oxide particles or hemorrhage. (B) Rhodamine B fluorescence (red) of iron oxide particles and DAPI staining of nuclei (blue). (A1, B1) Tendon lesions injected with serum only. (A2, B2) Tendon lesions injected with labeled MSCs (MSC inj.). Black arrows point at accumalations of Prussian blue staining, partly displaying fibroblast-like shapes; white arrows point at Rhodamine B-positive particles associated with cell nuclei, which were considered as labeled MSCs; gray arrows point at isolated fluorescent particles. Black scale bars: 100 μm, white scale bars: 20 μm. Circle and rhomb in the boxplot show outliers.

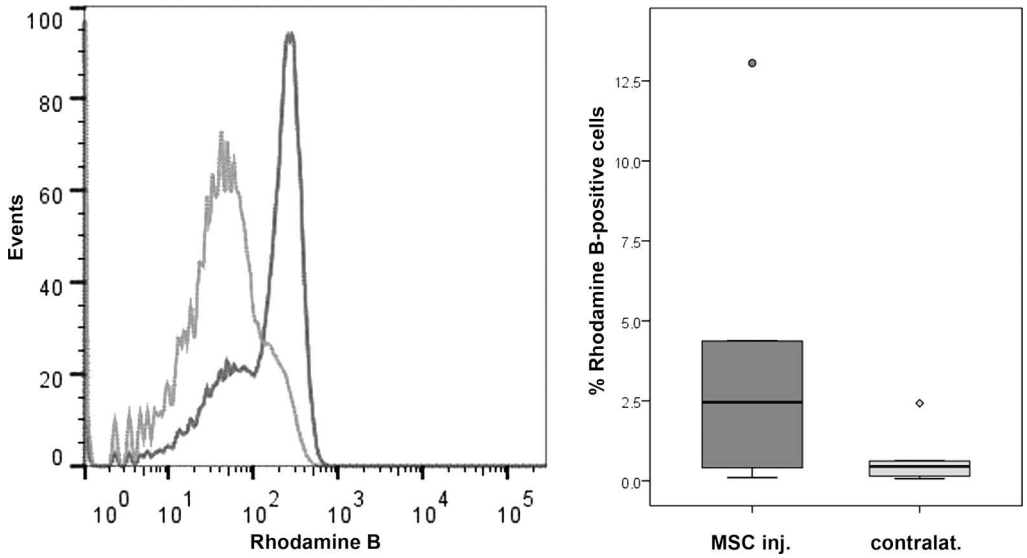

Figure 5. Flow cytometry of tendon lesions. Representative histogram displaying the number of events versus Rhodamine B fluorescence intensity. The light gray line represents unstained control cells, and the dark gray line represents the cells recovered from a tendon lesion 3 weeks after injection of labeled MSCs. The boxplot displays the Rhodamine B-positive percentage of cells recovered from the tendon lesions injected with labeled MSCs (MSC inj.) and the contralateral tendons injected with serum only. Circle and rhomb show outliers.

SPIO-induced hypointense artifacts observed in MRI do not always show a specific appearance and can therefore be confused with other hypointense tissue areas. This can be of particular importance for cell tracking in tendons, as their healthy fibers naturally display hypointense signal in standard MRI sequences. In our previous work, we aimed to validate the specificity of the cell tracking technique by comparing blinded subjective evaluation and quantitative assessment. While recognition of artifacts by blinded observers was surprisingly good, the results still underlined the importance of signal intensity quantification (6). In the current study, the latter was confirmed to be constantly low (data not shown), and results were additionally validated using the magic angle technique for MRI (unpublished data) (9), indicating a reliable identification of SPIO-artifacts and artifact volume.

However, even if artifacts can be correctly related to the presence of SPIO particles, MRI does not provide information on whether these SPIO particles are consistently labeling the cells in question. Moreover, when interpreting artifact localization, it should be acknowledged that its dimensions depend on the amount of iron. Therefore, it remains possible that at high SPIO concentrations, the area covered by artifact exceeds the exact localization of labeled cells (6). The latter is likely to occur during the first days after cell labeling only (6), but eventually both issues can only be clarified on the basis of corresponding histology.

Furthermore, MRI is not suitable to investigate systemic distribution of labeled cells. At least for large animals, this is due to the fact that scans need to be restricted to certain areas of the body. Moreover, this is also due to the limited sensitivity when it comes to distribution and dilution of labeled cells. Regarding the latter, 100,000 MSCs labeled at the same concentration as used in this study can be distinguished from agar gel by low-field MRI, but lower concentrations cannot be identified reliably (6). Correspondingly, using 3-T high-field MRI, 10,000 SPIO-labeled MSCs were still visible in agar gel, but differences in MRI signal were less pronounced compared to 100,000 or more cells (29). Therefore, it can be assumed that only accumulations of roughly 100,000 labeled cells or more can be visualized under in vivo conditions. For more sensitive cell detection, further techniques need to be applied.

Despite its limitations, MRI documented the distribution of artifact within the lesion and surrounding tissue over time. Artifact was constantly found within the tendon lesion, but distribution in the peritendineous tissue was also evident, suggesting partial leakage of MSCs. While it could be speculated that this was due to the artificial character of the tendon lesions, as the peritendineum was incised during their induction, we observed similar artifact distribution in patients with natural tendon core lesions (6). Furthermore, this finding is in accordance with a recent study (19) showing that cell application has yet to be optimized.

Histology, while also being limited to specific tissue areas, gives insight into tissue microstructure and allows to identify single cells. Here the major challenge is the appropriate labeling and staining. Prussian blue staining

offers the advantage that it allows the assessment by light microscopy, facilitating an evaluation of its localization within the tissue microstructure. Staining appears to be used as a gold standard for the identification of SPIO particles in tissue sections (29,38) and was discussed as being suitable to confirm that MRI artifacts correspond to SPIO rather than hemorrhage (29). However, in the context of MRI cell tracking, it is often neglected that Prussian blue staining is not specific for the iron oxide particles used for cell labeling. Prussian blue staining occurs in the presence of Fe(III) and is traditionally used for the identification of red blood cell degradation and siderophages. In forensic medicine, it is helpful to determine wound age (16). Consequently, Prussian blue staining could occur at previously injured tissue regions irrespective of the presence of SPIO particles. Therefore, in the current study, control samples of injured tissue were prepared to gain more insight into the specificity of the staining for SPIO detection. In fact, the control injured tissue also displayed positive staining, although not as extensive as found in the animals treated with SPIO-labeled MSCs. Based on that, while it still appears reasonable that Prussian blue staining of cellular structures is correlated with the presence of labeled cells, this staining alone does not ultimately prove the presence of labeled cells.

In the current study, evaluation of the simultaneous Rhodamine B labeling could confirm the presence of labeled cells within the tendon lesions. However, as was to be expected considering that part of the Prussian blue staining was due to previous hemorrhage, Rhodamine B-labeled cells were found in lower quantities than Prussian blue staining in corresponding slides, especially at week 3. This finding corresponds to the previous study performed in sheep using simultaneous green fluorescent protein transfection and SPIO labeling of MSCs. Here particularly 2 weeks after cell application, less GFP staining was observed not only compared to week 1 but also compared to corresponding Prussian blue-stained sections (29). The authors interpreted this finding to be due to the occurrence of free SPIO particles, which is a possibility that should not be dismissed in the current study either.

While transfected GFP most reliably identifies the actual transplanted cells, its expression is not related to the SPIO particles; thus, using this technique cannot finally explore their fate. Particularly, discrepancies between GFP expression and Prussian blue staining could merely be related to the presence of blood cell degradation products staining positive for the latter. In the current study, SPIO particles were directly conjugated to Rhodamine B and only rarely occurred without associated nuclei. This suggests that even after 24 weeks the occurrence of free SPIO particles is not a major issue. Nevertheless, it is still possible that SPIO particles are not located in the cytoplasm of the initially labeled MSCs but in macrophages that have phagocytosed free particles. On the basis of immunohistochemical costaining of macrophages in preliminary experiments as well as on the general morphological differences of macrophages and MSCs, we believe that macrophages do not make a major contribution to the labeled cell population. However, simultaneous detection of GFP and SPIO labeling would be required to prove this assumption.

As the detection of Rhodamine B-positive cells proved to be more specific than the detection of Prussian blue-positive cells, it would have provided valuable information to quantify the occurrence of labeled cells based on their fluorescence instead of Prussian blue staining. However, partially occurring autofluorescence of collagen fibers and erythrocytes in the histological sections hampered a clear distinction of all labeled cells. Therefore, to prevent false-positive results, we restricted the assessment of Rhodamine B-positive cells in histological sections to a descriptive evaluation of the cells that could clearly be recognized. However, flow cytometry of cells released from corresponding tissue samples at week 3 supported the subjective evaluation of tissue sections and demonstrated higher median numbers of labeled cells in the MSC-injected lesions and lower median numbers of labeled cells in the contralateral lesions.

The fact that small numbers of labeled cells could be found at the contralateral lesion sites that had not received MSC injections is not astonishing, given that MSCs are also found in the peripheral blood within the first hours after their application. This was not only observed in the current study but also corresponds to the findings in previous work (12). In both studies, it was also evident that numbers of labeled cells within the peripheral blood decreased within 7 days after their application. This leads to the hypothesis that the cells mainly enter the blood circulation around the time of injection, which can likely be due to damage of small blood vessels by the injection cannula. Correspondingly, results of a scintigraphic study showed that more than half of the cell label initially found at the injection site is lost during the first 24 h (36). Once having entered the blood circulation, MSCs are likely to home to other injury sites mediated by chemokines and integrins, which has repeatedly been described and investigated (35). However, our finding of labeled cells relocating to other injury sites after local application in tendon lesions is new compared to previous studies (12,21,25).

While interesting, the clinical relevance of this finding is not finally clear, as local injection still appears to be the most effective delivery route for treatment of tendon lesions (36). Nevertheless, it should be considered that MSC distribution and persistence are not exclusively local when evaluating the safety of the therapy. Furthermore, the finding is of relevance for the design of studies on MSC treatment efficacy. In order to limit

the number of animals required, it is current practice to use lesions induced in the contralateral limb of the same animal as negative controls (11,14,30). However, some of the MSCs injected into one limb could relocate to the contralateral limb, which then does not represent a completely reliable negative control, although the effect of a few relocated cells is presumably low.

Most importantly, the current findings strongly suggest that MSCs remain at the site of tendon injury after local application for a period of at least 24 weeks. This assumption is supported by the constantly low signal of artifacts found at the injection site, but more importantly, labeled cells could be identified in the corresponding histological sections. The number of cells concentrated within the tendon lesion decreased over time, as indicated by the decreasing volume of the artifacts in MRI as well as observed in the histological sections. Nevertheless, given that at week 24 several cells could still be identified in separate tissue sections, each representing only a very small percentage of the whole tendon lesion, the results suggest that part of the locally applied MSCs remain viable and integrate within the injured tissue. However, it should not be neglected that there is also cell distribution to distant locations as well as partial leakage of injected cells into peritendineous tissues. Future studies still need to reveal the exact percentage of cells surviving at the lesion site after an optimized application procedure.

It should also be acknowledged that cell-labeling agents, including SPIO, can have side effects (3,4), which can hamper the observation of physiological processes in labeled cells and their environment. Moreover, the disease model used could have an impact on MSC behavior, particularly on cell survival and homing. The two most frequently used techniques for tendon lesion induction in large animals are collagenase application (24), which can induce massive inflammation, and surgical disruption of tendon tissue (31), which physically destroys large amounts of tendon fibers. The model used in the current study combined both techniques, using a low dose of collagenase and very limited tissue disruption, aiming to minimize the disadvantages of both approaches. In addition to that, it remains to be considered that tendon healing and MSC distribution in fore- and hindlimbs may not be identical (17). However, MRI findings in the current study were very similar to those in our previous study in equine patients with natural forelimb tendon lesions.

Therefore, it could be assumed that the model used largely reflects the natural condition; thus, the present findings could be of high practical relevance. The results of the current study appear to be relevant with respect to the potential mechanisms of action of MSCs in tendon regeneration, as persistence of the cells over a long period of time would potentially allow them to continuously influence local regenerative processes.

ACKNOWLEDGMENTS: The authors thank Dr. Claudia Gittel, Large Animal Clinic for Surgery, and Dr. Kristin Mueller, Institute of Veterinary Pathology, both at the University of Leipzig, for their help and scientific input. Furthermore, the authors thank the whole team of the Large Animal Clinic for Surgery, University of Leipzig, for helping with the in vivo experiments, as well as the team of the Institute of Veterinary Pathology, University of Leipzig, for preparing the histological sections. The authors also acknowledge Dr. Ingrid Vervuert, Institute of Animal Nutrition, Nutrition Diseases and Dietetics, University of Leipzig, for providing access to control samples. The work presented in this article was made possible by funding from the German Federal Ministry of Education and Research (BMBF 1315883) and the Saxon Ministry of Science and the Fine Arts (SMWK). The authors declare no conflicts of interest.

REFERENCES

1. Addicott, B.; Willman, M.; Rodriguez, J.; Padgett, K.; Han, D.; Berman, D.; Hare, J. M.; Kenyon, N. S. Mesenchymal stem cell labeling and in vitro MR characterization at 1.5 T of new SPIO contrast agent: Molday ION Rhodamine-B. Contrast Media Mol. Imaging 6(1):7–18; 2011.
2. Andreas, K.; Georgieva, R.; Ladwig, M.; Mueller, S.; Notter, M.; Sittinger, M.; Ringe, J. Highly efficient magnetic stem cell labeling with citrate-coated superparamagnetic iron oxide nanoparticles for MRI tracking. Biomaterials 33(18):4515–4525; 2012.
3. Astanina, K.; Simon, Y.; Cavelius, C.; Petry, S.; Kraegeloh, A.; Kiemer, A. K. Superparamagnetic iron oxide nanoparticles impair endothelial integrity and inhibit nitric oxide production. Acta Biomater. 10(11):4896–4911; 2014.
4. Banda, N. K.; Mehta, G.; Chao, Y.; Wang, G.; Inturi, S.; Fossati-Jimack, L.; Botto, M.; Wu, L.; Moghimi, S. M.; Simberg, D. Mechanisms of complement activation by dextran-coated superparamagnetic iron oxide (SPIO) nanoworms in mouse versus human serum. Part Fibre Toxicol. 11:64; 2014.
5. Becerra, P.; Valdes Vazquez, M. A.; Dudhia, J.; Fiske-Jackson, A. R.; Neves, F.; Hartman, N. G.; Smith, R. K. Distribution of injected technetium(99m)-labeled mesenchymal stem cells in horses with naturally occurring tendinopathy. J. Orthop. Res. 31(7):1096–1102; 2013.
6. Berner, D.; Brehm, W.; Gerlach, K.; Gittel, C.; Offhaus, J.; Paebst, F.; Scharner, D.; Burk, J. Longitudinal cell tracking and simultaneous monitoring of tissue regeneration after cell treatment of natural tendon disease by low-field magnetic resonance imaging. Stem Cells Int. 2016:1207190; 2016.
7. Bourzac, C. A.; Koenig, J. B.; Link, K. A.; Nykamp, S. G.; Koch, T. G. Evaluation of ultrasmall superparamagnetic iron oxide contrast agent labeling of equine cord blood and bone marrow mesenchymal stromal cells. Am. J. Vet. Res. 75(11):1010–1017; 2014.
8. Brehm, W.; Burk, J.; Delling, U. Application of stem cells for the treatment of joint disease in horses. Methods Mol. Biol. 1213:215–228; 2014.
9. Burk, J.; Horstmeier, C.; Ahrberg, A. B.; Hillmann, A.; Winter, K.; Brehm, W. Longitudinal cell tracking by magnetic resonance imaging following treatment of induced tendon lesions. Tissue Eng. Part A 21(Suppl. 1):50; 2015.
10. Burk, J.; Ribitsch, I.; Gittel, C.; Juelke, H.; Kasper, C.; Staszyk, C.; Brehm, W. Growth and differentiation characteristics of equine mesenchymal stromal cells derived from different sources. Vet. J. 195(1):98–106; 2013.
11. Caniglia, C. J.; Schramme, M. C.; Smith, R. K. The effect of intralesional injection of bone marrow derived mesenchymal

stem cells and bone marrow supernatant on collagen fibril size in a surgical model of equine superficial digital flexor tendonitis. Equine Vet. J. 44(5):587–593; 2012.
12. Carvalho, A. M.; Yamada, A. L.; Golim, M. A.; Alvarez, L. E.; Hussni, C. A.; Alves, A. L. Evaluation of mesenchymal stem cell migration after equine tendonitis therapy. Equine Vet. J. 46(5):635–638; 2014.
13. Crabbe, A.; Vandeputte, C.; Dresselaers, T.; Sacido, A. A.; Verdugo, J. M.; Eyckmans, J.; Luyten, F. P.; Van, L. K.; Verfaillie, C. M.; Himmelreich, U. Effects of MRI contrast agents on the stem cell phenotype. Cell Transplant. 19(8):919–936; 2010.
14. Crovace, A.; Lacitignola, L.; Rossi, G.; Francioso, E. Histological and immunohistochemical evaluation of autologous cultured bone marrow mesenchymal stem cells and bone marrow mononucleated cells in collagenase-induced tendinitis of equine superficial digital flexor tendon. Vet. Med. Int. 2010:250978; 2010.
15. Delling, U.; Brehm, W.; Metzger, M.; Ludewig, E.; Winter, K.; Julke, H. In vivo tracking and fate of intraarticularly injected superparamagnetic iron oxide particle-labeled multipotent stromal cells in an ovine model of osteoarthritis. Cell Transplant. 24(11):2379–2390; 2015.
16. Dettmeyer, R. B. Forensic histopathology. Berlin–Heidelberg (Germany): Springer-Verlag; 2011.
17. Estrada, R. J.; van Weeren, P. R.; van De Lest, C. H.; Boere, J.; Reyes, M.; Ionita, J. C.; Estrada, M.; Lischer, C. J. Comparison of healing in forelimb and hindlimb surgically induced core lesions of the equine superficial digital flexor tendon. Vet. Comp. Orthop. Traumatol. 27(5):358–365; 2014.
18. European Medicines Agency; Committee For Advanced Therapies (CAT). Reflection paper on in-vitro cultured chondrocyte containing products for cartilage repair of the knee. http://www.ema.europa.eu; 2010.
19. Geburek, F.; Mundle, K.; Conrad, S.; Hellige, M.; Walliser, U.; van Schie, H. T.; van Weeren, R.; Skutella, T.; Stadler, P. M. Tracking of autologous adipose tissue-derived mesenchymal stromal cells with in vivo magnetic resonance imaging and histology after intralesional treatment of artificial equine tendon lesions—A pilot study. Stem Cell Res. Ther. 7(1):21; 2016.
20. Guest, D. J.; Smith, M. R.; Allen, W. R. Monitoring the fate of autologous and allogeneic mesenchymal progenitor cells injected into the superficial digital flexor tendon of horses: Preliminary study. Equine Vet. J. 40(2):178–181; 2008.
21. Guest, D. J.; Smith, M. R.; Allen, W. R. Equine embryonic stem-like cells and mesenchymal stromal cells have different survival rates and migration patterns following their injection into damaged superficial digital flexor tendon. Equine Vet. J. 42(7):636–642; 2010.
22. Hillmann, A.; Ahrberg, A. B.; Brehm, W.; Heller, S.; Josten, C.; Paebst, F.; Burk, J. Comparative characterization of human and equine mesenchymal stromal cells: A basis for translational studies in the equine model. Cell Transplant. 25(1):101–124; 2016.
23. Julke, H.; Veit, C.; Ribitsch, I.; Brehm, W.; Ludewig, E.; Delling, U. Comparative labeling of equine and ovine multipotent stromal cells with superparamagnetic iron oxide particles for magnetic resonance imaging in vitro. Cell Transplant. 24(6):1111–1125; 2015.
24. Keg, P. R.; van den Belt, A. J.; Merkens, H. W.; Barneveld, A.; Dik, K. J. The effect of regional nerve blocks on the lameness caused by collagenase induced tendonitis in the mid-metacarpal region of the horse: A study using gait analysis, and ultrasonography to determine tendon healing. Zentralbl. Veterinarmed. A 39(5):349–364; 1992.
25. Lacitignola, L.; Staffieri, F.; Rossi, G.; Francioso, E.; Crovace, A. Survival of bone marrow mesenchymal stem cells labelled with red fluorescent protein in an ovine model of collagenase-induced tendinitis. Vet. Comp. Orthop. Traumatol. 27(3):204–209; 2014.
26. Lui, P. P.; Maffulli, N.; Rolf, C.; Smith, R. K. What are the validated animal models for tendinopathy? Scand. J. Med. Sci. Sports 21(1):3–17; 2011.
27. Paebst, F.; Piehler, D.; Brehm, W.; Heller, S.; Schroeck, C.; Tarnok, A.; Burk, J. Comparative immunophenotyping of equine multipotent mesenchymal stromal cells: An approach toward a standardized definition. Cytometry A 85(8):678–687; 2014.
28. Patterson-Kane, J. C.; Becker, D. L.; Rich, T. The pathogenesis of tendon microdamage in athletes: The horse as a natural model for basic cellular research. J. Comp. Pathol. 147(2–3):227–247; 2012.
29. Scharf, A.; Holmes, S.; Thoresen, M.; Mumaw, J.; Stumpf, A.; Peroni, J. Superparamagnetic iron oxide nanoparticles as a means to track mesenchymal stem cells in a large animal model of tendon injury. Contrast Media Mol. Imaging 10(5): 388–397; 2015.
30. Schnabel, L. V.; Lynch, M. E.; van der Meulen, M. C.; Yeager, A. E.; Kornatowski, M. A.; Nixon, A. J. Mesenchymal stem cells and insulin-like growth factor-I gene-enhanced mesenchymal stem cells improve structural aspects of healing in equine flexor digitorum superficialis tendons. J. Orthop. Res. 27(10):1392–1398; 2009.
31. Schramme, M.; Hunter, S.; Campbell, N; Blikslager A; Smith R. A surgical tendonitis model in horses: Technique, clinical, ultrasonographic and histological characterisation. Vet. Comp. Orthop. Traumatol. 23(4):231–239; 2010.
32. Smith, R. K.; Korda, M.; Blunn, G. W.; Goodship, A. E. Isolation and implantation of autologous equine mesenchymal stem cells from bone marrow into the superficial digital flexor tendon as a potential novel treatment. Equine Vet. J. 35(1):99–102; 2003.
33. Smith, R. K.; McIlwraith, C. W. Consensus on equine tendon disease: Building on the 2007 Havemeyer symposium. Equine Vet. J. 44(1):2–6; 2012.
34. Smith, R. K.; Werling, N. J.; Dakin, S. G.; Alam, R.; Goodship, A. E.; Dudhia, J. Beneficial effects of autologous bone marrow-derived mesenchymal stem cells in naturally occurring tendinopathy. PLoS One 8(9):e75697; 2013.
35. Sohni, A.; Verfaillie, C. M. Mesenchymal stem cells migration homing and tracking. Stem Cells Int. 2013:130763; 2013.
36. Sole, A.; Spriet, M.; Padgett, K. A.; Vaughan, B.; Galuppo, L. D.; Borjesson, D. L.; Wisner, E. R.; Vidal, M. A. Distribution and persistence of technetium-99 hexamethyl propylene amine oxime-labelled bone marrow-derived mesenchymal stem cells in experimentally induced tendon lesions after intratendinous injection and regional perfusion of the equine distal limb. Equine Vet. J. 45(6):726–731; 2013.
37. U.S. Department of Health and Human Services; Food and Drug Administration; Center for Biologics Evaluation and Research. Guidance for industry: Preclinical assessment of investigational cellular and gene therapy products. http://www.fda.gov; 2013.
38. Yang, Y.; Zhang, J.; Qian, Y.; Dong, S.; Huang, H.; Boada, F. E.; Fu, F. H.; Wang, J. H. Superparamagnetic iron oxide is suitable to label tendon stem cells and track them in vivo with MR imaging. Ann. Biomed. Eng. 41(10):2109–2119; 2013.